Flux distributions as robust diagnostics of stratosphere-troposphere exchange

Clara Orbe,[1] Mark Holzer,[1,2] and Lorenzo M. Polvani[1,3]

Received 23 June 2011; revised 31 October 2011; accepted 1 November 2011; published 7 January 2012.

[1] We perform the first analysis of stratosphere-troposphere exchange in terms of distributions that partition the one-way flux across the thermal tropopause according to stratospheric residence time τ and the regions where air enters and exits the stratosphere. These distributions robustly quantify one-way flux without being rendered ill defined by the short-τ eddy-diffusive singularity. Diagnostics are computed with an idealized circulation model with topography only in the Northern Hemisphere (NH) run under perpetual NH winter conditions. Suitable integrations of the flux distribution are used to determine the stratospheric mean residence time $\bar{\tau}$ and the mass fraction of the stratosphere in any given residence time interval. We find that the largest mass fraction is destined for isentropic cross-tropopause transport, with one-way fluxes that are sustained over a broad range of residence times. Air exiting the stratosphere in the winter hemisphere has significantly longer mean residence times than air exiting in the summer hemisphere because the winter hemisphere has a deeper circulation and stronger eddy diffusion. We also explore the sensitivity of the stratosphere-troposphere exchange to changes in the circulation by increasing the amplitude of the topography. The resulting more vigorous residual mean circulation dominates over increased eddy diffusion, leading to decreased $\bar{\tau}$ except for air exiting at high NH latitudes, for which $\bar{\tau}$ increases. These findings underline that the flux distributions diagnose the integrated advective-diffusive tropopause-to-tropopause transport and not merely advection by the residual mean circulation.

Citation: Orbe, C., M. Holzer, and L. M. Polvani (2012), Flux distributions as robust diagnostics of stratosphere-troposphere exchange, *J. Geophys. Res.*, *117*, D01302, doi:10.1029/2011JD016455.

1. Introduction

[2] The chemical and radiative properties of the troposphere and lower stratosphere are strongly influenced by the stratosphere-troposphere exchange (STE) of mass and tracers [e.g., *Morgenstern and Carver*, 2001; *Park et al.*, 2004; *Jing et al.*, 2005; *Hegglin et al.*, 2006; *Pan et al.*, 2006, 2007]. Changes in STE with a changing climate will have important implications for the distribution of ozone, for the oxidizing capacity of the troposphere [e.g., *Kentarchos and Roelofs*, 2003], and hence for tropospheric air quality [e.g., *Stohl et al.*, 2000; *Cooper et al.*, 2005; *Hsu et al.*, 2005]. We emphasize, however, that our study does not focus on the net flux of ozone; instead we develop tracer-independent diagnostics of STE.

[3] Recent simulations [*Hegglin and Shepherd*, 2009; *Zeng et al.*, 2010] using comprehensive general circulation models with coupled stratospheric chemistry predict that the Brewer-Dobson circulation (BDC) will increase over the 21st century leading to increased stratosphere-to-troposphere (S → T) ozone fluxes, increased surface ultraviolet radiation exposure, and increased surface ozone levels. It is therefore important to obtain a fundamental, quantitative understanding of cross-tropopause transport.

[4] Because of eddy-diffusive mixing, large cross-tropopause tracer gradients can lead to significant tracer transport even if the net mass flux is zero [*Gettelman and Sobel*, 2000]. The net air mass flux [*Holton et al.*, 1995; *Appenzeller et al.*, 1996; *James et al.*, 2003; *Olsen et al.*, 2004] is therefore not a useful transport diagnostic. In recognition of this fact, investigators have focused on the one-way (also called "gross") S → T and T → S fluxes [*Stohl et al.*, 2000; *Wernli and Bourqui*, 2002]. While it was not recognized from the outset, it is now clear that these one-way fluxes are fundamentally ill defined and, in fact, singular in the continuum limit, unless additional constraints on either entry/exit locations and/or residence time are imposed [*Hall*

[1]Department of Applied Physics and Applied Mathematics, Columbia University, New York, New York, USA.
[2]Department of Applied Mathematics, School of Mathematics and Statistics, University of New South Wales, Sydney, New South Wales, Australia.
[3]Department of Earth and Environmental Sciences, Columbia University, New York, New York, USA.

0148-0227/12/2011JD016455

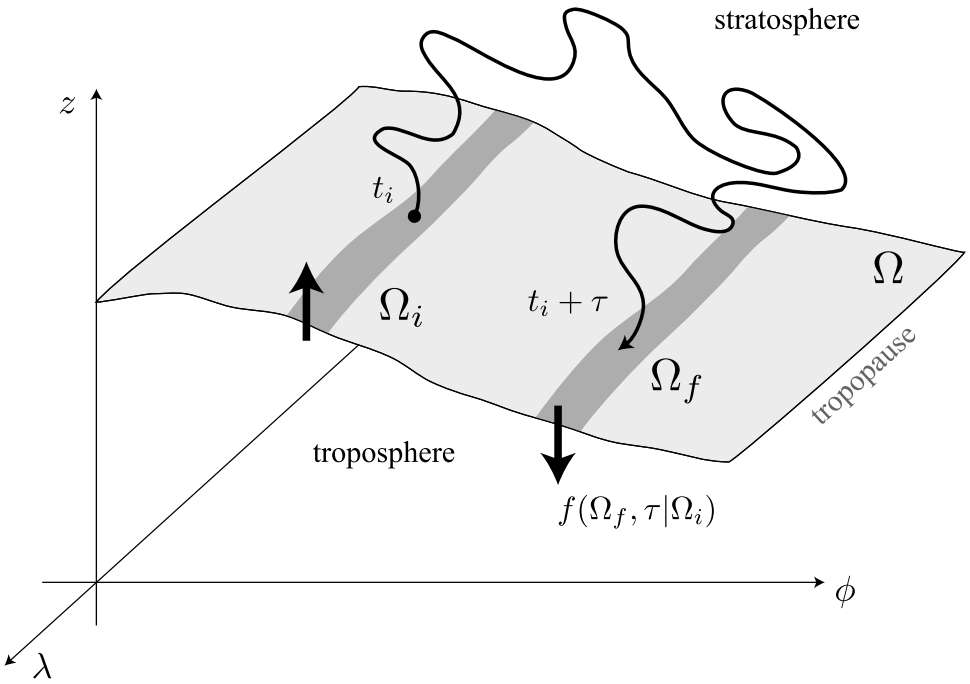

Figure 1. Schematic illustration of tropopause-to-tropopause transport through the stratosphere. The axes are longitude λ, latitude ϕ, and height z. Air is labeled with tracer $\mathcal{G}$ as it enters the stratosphere through tropopause patch Ω_i during $(t_i, t_i + dt_i)$. The flux of this labeled air out of the stratosphere through tropopause patch Ω_f, after a residence time in the interval $(\tau, \tau + d\tau)$, is given by $f(\Omega_f, \tau\,|\Omega_i)d\tau$ in the ensemble mean. Zero–mixing ratio boundary conditions on the tropopause prevent any return flux of labeled air from the troposphere, ensuring that f is the one-way S→ T flux density.

and Holzer, 2003; *Primeau and Holzer*, 2006]. Residence time here refers to the time spent in the stratosphere between successive crossings of the tropopause.

[5] The singular nature of the one-way fluxes arises physically from the quasi-random nature of eddy diffusion at the shortest resolved length and time scales. Although the singularity can be avoided by demanding that fluid elements stay for at least a threshold residence time on the other side of the tropopause before recrossing, the one-way cross-tropopause flux is in practice found to be a rapidly changing function of such a threshold time [*Wernli and Bourqui*, 2002; *Bourqui*, 2006]. This sensitivity to residence time explains the widely divergent estimates of STE fluxes reported in the literature [*Gettelman and Sobel*, 2000; *Hall and Holzer*, 2003].

[6] The one-way cross-tropopause flux is nevertheless an appropriate and powerful transport diagnostic once it is understood that this flux must be considered to be a distribution over residence time, and not a single number [*Hall and Holzer*, 2003]. One needs to partition (or "bin") the one-way flux with respect to residence time, τ, and with respect to the regions where the tropopause is being crossed. The resulting one-way flux distribution f is the fundamental STE diagnostic at the heart of this study.

[7] The distribution f contains a wealth of information on STE, which is conveniently summarized in terms of a number of moments such as the mean stratospheric residence time $\bar{\tau}$ and the mass fraction μ of the stratosphere that enters and exits through specified regions of the tropopause. These moments are mathematically well-defined quantities that do not suffer from the diffusive singularity of f as $\tau \to 0$. Indeed, following *Primeau and Holzer* [2006], we will first use f to compute an integrable joint distribution of residence time and entry/exit location and then compute $\bar{\tau}$ and μ.

[8] Following an exposition of the theory and methodology, we illustrate the utility of f and some of its key properties for quantifying STE with the results from an idealized GCM [*Held and Suarez*, 1994; *Gerber and Polvani*, 2009]. The sensitivity of our STE diagnostics to circulation changes is also explored within the context of the idealized GCM. We emphasize, however, that the flux density diagnostics can straightforwardly be computed using any circulation model capable of carrying conserved passive tracers.

2. Theory: Flux Distribution and Residence Time Partitioned Mass

[9] In order to quantify STE we must first define a tropopause, denoted throughout by Ω. To partition the one-way flux according to where air enters and exits the stratosphere, we tile the tropopause with patches. Patches where we track the one-way entry of air into the stratosphere are denoted by Ω_i, and patches where we track the one-way exit of air are denoted by Ω_f (see Figure 1). (We note that on both patches there will also be one-way flux in the opposite direction, resulting in the net flux of air, and that when transport from Ω_i back to Ω_i is considered, one has $\Omega_f = \Omega_i$.) To track air parcels during their transit from Ω_i to Ω_f we use the boundary propagator Green function $\mathcal{G}$ (which has dimensions of inverse time). Physically, $\mathcal{G}(\mathbf{r}, t|\Omega_i, t_i)dt_i$ is the mass fraction

of air at position $\mathbf{r}$ and time t that had last Ω_i contact during $(t_i, t_i + dt_i)$. One may think of $\mathcal{G}$ as a label that is applied to air on Ω_i during $(t_i, t_i + dt_i)$ and for convenience we refer to air labeled by $\mathcal{G}(\mathbf{r}, t|\Omega_i, t_i)$ as "(Ω_i, t_i) air".

[10] The boundary propagator $\mathcal{G}$ is computed as the passive tracer response to a pulse in mixing ratio applied during $(t_i, t_i + dt_i)$ over tropopause patch Ω_i that satisfies the source-free advection–diffusion equation

$$\frac{\partial}{\partial t}(\rho\mathcal{G}) + \nabla\cdot\mathbf{J} = 0, \tag{1}$$

where $\mathbf{J}$ is the advective-diffusive mass flux of $\mathcal{G}$, and ρ is the density of air. For the generic case of advection with velocity $\mathbf{u}$ and Fickian diffusion with diffusivity tensor $\mathbf{K}$, we have $\mathbf{J} = (\rho\mathbf{u} - \rho\mathbf{K}\nabla)\mathcal{G}$. The boundary conditions for $\mathcal{G}$ are

$$\mathcal{G}(\mathbf{r}_\Omega, t|\Omega_i, t_i) = \Delta^2(\mathbf{r}_\Omega, \Omega_i)\delta(t - t_i), \tag{2}$$

where $\delta(t - t_i)$ is the usual Dirac delta function and the surface mask $\Delta^2(\mathbf{r}_\Omega, \Omega_i) = 1$ if tropopause point $\mathbf{r}_\Omega$ lies on patch Ω_i, and $\Delta^2(\mathbf{r}_\Omega, \Omega_i) = 0$ otherwise. Note that a boundary condition of zero applies to the entire tropopause for $t > t_i$. This ensures that the $\mathcal{G}$ label is removed when (Ω_i, t_i) air makes contact with the tropopause for $t > t_i$.

[11] The area-averaged S → T mass flux of (Ω_i, t_i) air through patch Ω_f that has resided in the stratosphere for a time in the interval $(\tau, \tau + d\tau)$ is formally given by

$$f(\Omega_f, t_i + \tau|\Omega_i, t_i)d\tau = d\tau\frac{1}{A(\Omega_f)}\int_{\Omega_f} d^2r\,\hat{\mathbf{n}}\cdot\mathbf{J}(\mathbf{r}, t_i + \tau|\Omega_i, t_i), \tag{3}$$

where $\hat{\mathbf{n}}$ is the surface normal of the tropopause and $A(\Omega_f)$ is the area of Ω_f. The boundary conditions (2) ensure that there is no return flux of Ω_i air from the troposphere so that f is the one-way, or gross, S → T flux. The flux f has the same dimensions as $\mathbf{J}$ (mass area^{-1} time^{-2}) and is therefore a flux-density distribution that partitions the flux of (Ω_i, t_i) air through Ω_f according to residence time, τ. Note that conservation of mass demands that the flow rate $A(\Omega_f)f(\Omega_f, t_i + \tau|\Omega_i, t_i)d\tau$ is both the rate with which Ω_i air in the residence time interval $(\tau, \tau + d\tau)$ exits through Ω_f at time $t_f = t_i + \tau$, and also the rate with which the same air entered through Ω_i at time t_i. Thus, the flux density not only quantifies the $\Omega_i \to \Omega_f$ S → T flux exiting through Ω_f, but $fA(\Omega_f)/A(\Omega_i)$ is also the T → S flux entering through Ω_i, per unit residence time.

[12] Given the flux density distribution f, it is natural to define the cumulative flux distribution $\mathcal{F}(\Omega_f, \tau^*|\Omega_i, t_i) \equiv \int_{\tau^*}^{\infty} d\tau f(\Omega_f, t_i + \tau|\Omega_i, t_i)$, which is the flux of (Ω_i, t_i) air with residence time τ and longer that exits through Ω_f. The cumulative flux $\mathcal{F}$ has dimensions (mass area^{-1} time^{-1}). Because of eddy diffusion, both f and $\mathcal{F}$ are singular at $\tau = 0$ for overlapping patches Ω_i and Ω_f. For the case of Fickian diffusion, $f \sim \tau^{-3/2}$ and $\mathcal{F} \sim \tau^{-1/2}$ in the limit of small τ [*Hall and Holzer*, 2003; *Primeau and Holzer*, 2006].

[13] It is interesting to ask what fraction of the stratosphere undergoes $\Omega_i \to \Omega_f$ transport in any given residence time interval. To this end, one can integrate the flux density f to obtain the integrable distribution $\mathcal{R}$ defined so that $\mathcal{R}(\tau, \Omega_i, \Omega_f)d\tau$ is the mass fraction of the stratosphere that has entered through Ω_i and is destined to exit through Ω_f after a $\Omega_i \to \Omega_f$ transit time in the interval $(\tau, \tau + d\tau)$, the transit time to Ω_f being the stratospheric residence time.

[14] *Primeau and Holzer* [2006] worked out the relationship between $\mathcal{R}$ and f for general time-varying flow, for which $\mathcal{R}$ can only be computed using a large number of tracers [*Holzer and Hall*, 2008]. Here we avoid the need for a large number of tracers by ensemble averaging over several realizations of the flow so that we can use a simple relationship derivable for steady flow. (For steady flow f and $\mathcal{R}$, and diagnostics derived therefrom, depend on time only through τ, and we omit the t_i dependence for ensemble averages.) The fact that the mass with residence time τ is flushed out of the stratosphere in time τ gives for steady flow that

$$\mathcal{R}(\tau, \Omega_i, \Omega_f) = \frac{1}{M}\,A(\Omega_f)f(\Omega_f, \tau|\Omega_i)\tau, \tag{4}$$

where M is the mean mass of the stratosphere. We note in passing that $\mathcal{R}$ also has the interpretation of being a domain integrated path density [*Holzer*, 2009a, 2009b].

[15] Because $\mathcal{R}$ partitions the finite mass of the stratosphere, it is integrable even when overlapping entry/exit patches introduce a zero-τ singularity, with the normalization

$$\sum_{\Omega_i}\sum_{\Omega_f}\int_0^\infty d\tau\,\mathcal{R}(\tau, \Omega_i, \Omega_f) = 1. \tag{5}$$

The distribution $\mathcal{R}$ is usefully summarized by its moments. The mass fraction, $\mu(\Omega_i, \Omega_f)$, of the stratosphere undergoing $\Omega_i \to \Omega_f$ transport is given by

$$\mu(\Omega_i, \Omega_f) \equiv \int_0^\infty d\tau\,\mathcal{R}(\tau, \Omega_i, \Omega_f), \tag{6}$$

and the mean $\Omega_i \to \Omega_f$ residence time is given by

$$\bar{\tau}(\Omega_i, \Omega_f) \equiv \frac{1}{\mu(\Omega_i, \Omega_f)}\int_0^\infty d\tau\,\tau\mathcal{R}(\tau, \Omega_i, \Omega_f). \tag{7}$$

[16] It is important to distinguish the mean residence time $\bar{\tau}$ from the stratospheric mean age Γ. First, note that for $\Omega_i = \Omega$ (the entire tropopause) $\mathcal{G}$ also has the interpretation of being the age spectrum [*Hall and Plumb*, 1994], and to the degree that the flow is statistically steady $\Gamma = \int_0^\infty \tau\mathcal{G}d\tau$. The mean age is the average time since last contact with the tropopause, and thus $\Gamma = 0$ at the tropopause. The mean residence time $\bar{\tau}$ is the average $\Omega_i \to \Omega_f$ transit time, where the weights of the average (7) partition the mass fraction of the entire stratosphere undergoing $\Omega_i \to \Omega_f$ transport according to residence time. Mean residence time cannot be deduced from mean age: $\Gamma(\mathbf{r})$ characterizes the transport from the tropopause to stratospheric point $\mathbf{r}$, while $\bar{\tau}$ includes the transit time from all interior locations back to the tropopause. To obtain the $\Omega_i \to \Omega_f$ transit time, one must diagnose the flux of Ω_i air (i.e., the flux of $\mathcal{G}$) out of the stratosphere through Ω_f. The mean residence time $\bar{\tau}$ cannot be computed from $\mathcal{G}$ itself because $\mathcal{G} = 0$ on the tropopause for $t > t_i$.

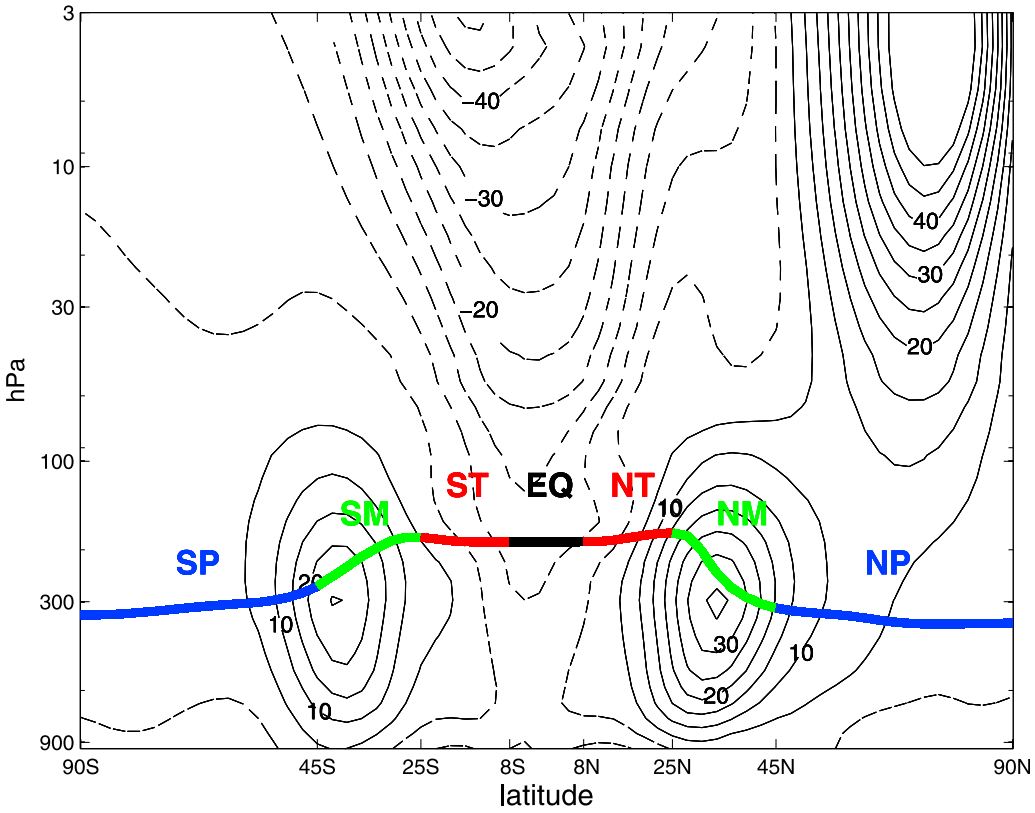

Figure 2. The time and zonal mean thermal tropopause (thick line) and contoured zonal winds. The contour interval is 5 m/s, and the zero and negative contours are dashed. Different colors at the tropopause label equal-area axisymmetric patches whose latitude bounds are labeled on the abscissa.

[17] The flux distribution f, defined by (3), is the fundamental transport diagnostic at the core of our analysis of STE, which we perform here in the context of an idealized GCM. Consistent with the idealized nature of the model atmosphere, we focus only on zonally averaged transport diagnostics, and use longitudinal tropopause strips for the patches Ω_i and Ω_f.

3. Methodology

3.1. The Model

[18] To illustrate our diagnostics we use a model of the dry atmosphere with idealized thermodynamic and momentum forcings as described by *Polvani and Kushner* [2002]. The temperature is linearly relaxed to an analytic equilibrium profile that is almost identical to that of *Held and Suarez* [1994], except for a factor to cause asymmetric temperature gradients between the hemispheres to better capture perpetual December-January-February (DJF) conditions. This Newtonian temperature relaxation yields baroclinic eddies in the troposphere and a polar vortex in the stratosphere, via an imposed cold anomaly above 100 hPa in the NH.

[19] To represent realistic stratospheric variability, we use the configuration of [*Gerber and Polvani*, 2009] (hereafter GP2009), which sets the polar vortex lapse rate to 4 K km^{-1} and imposes 3 km amplitude zonal wave number 2 topography in the NH midlatitudes centered at 45°N. GP2009 found that this combination of topography and thermal forcing produces a realistic frequency of stratospheric sudden warmings and realistic stratosphere-troposphere coupling. The small parameter space of the physics module lends itself well to sensitivity testing, a feature that we exploit in section 5. We note that the model does not include moist convection or seasonal variability nor is the resolution high enough to resolve gravity waves. However, our idealized model is more than adequate for illustrating our diagnostics. While our results will undoubtedly differ in quantitative detail from what a more comprehensive model would yield, the idealized model is sufficient to capture the key qualitative features of the one-way STE flux distribution.

[20] Our model integrates the global primitive equations in sigma coordinates using a pseudospectral method. We run at T42 horizontal resolution with 40 evenly spaced sigma levels up to 0.01 hPa. Spin-up to a statistically stationary state takes ~2000 days. An ensemble of five realizations of the Green function tracers is used to calculate our ensemble-averaged diagnostics. To generate the ensemble members, we perform a single long run initializing a new set of $\mathcal{G}$ tracers every 1000 days. As can be seen in Figure 2, the model's zonally averaged 2000 day climatology features a strong stratospheric polar jet centered around 60°N and 10 hPa, as well as tropospheric midlatitude jets.

[21] After spin-up we introduce our diagnostic $\mathcal{G}$ tracers that are passively advected by the flow; we use the advective form of the passive tracer equation. We use a semi-Lagrangian scheme for horizontal advection and a finite volume parabolic

scheme for vertical advection. No explicit diffusion is applied to tracers, but for vorticity, divergence, and temperature the model applies scale-selective horizontal hyperdiffusion of the form ∇^8. To correct for the relatively poor conservation properties of the semi-Lagrangian scheme, we use the model's built-in global "mass fixer," which scales the tracer field after every application of the advection operator to ensure that the global tracer mass remains unchanged by advection.

[22] Computing our diagnostics without the global mass fixer lengthens stratospheric mean residence time by 10%–15% without changing the qualitative character of the results. Of course a global rescaling cannot correct local errors in the flux, which we simply accept here along with the limitations of an idealized atmosphere for the purposes of illustrating the qualitative character of our new STE diagnostics.

3.2. The Diagnostic Tracers

[23] We identify the tropopause using the standard World Meteorological Organization (WMO) definition [*WMO*, 1957]: The thermal tropopause is located at the lowest model level where the lapse rate decreases to 2 K km^{-1}, with no increase for 2 km above that. This thermal tropopause is computed online for each time step and at every grid point. Thus defined, we would only capture the lowermost tropopause in the case of multiple tropopauses, but our resolution is too coarse to resolve any small-scale tropopause folds. It is worth noting, however, that our formulation naturally captures the one-way flux across any surface that separates tropospheric air from stratospheric air, even if that surface is multiply connected with isolated bubbles of air from one domain embedded in the other domain. Using suitable masks to identify all grid points in the tropopause allows one to compute the desired one-way flux as outlined in Appendix A.

[24] In order to partition the cross-tropopause flux according to where air enters the stratosphere, we tile the tropopause with seven equal-area, axisymmetric patches Ω_i as shown in Figure 2. We use two-letter subscripts to identify Ω_i. The patch straddling the equator from 8°S to 8°N is Ω_{EQ}, and for the other patches, the first letter identifies the hemisphere (N or S) and the second letter, the region: T for tropical (8° to 25°), M for subtropical to midlatitudes (25° to 45°), and P for mid to polar latitudes (45° to poles).

[25] For each integration starting at t_i we carry seven passive tracers $\mathcal{G}(\mathbf{r}, t|\Omega_i, t_i)$, one for each Ω_i. In practice the boundary conditions (2) are enforced as follows: The δ function is broadened to a square pulse of duration Δt_P = 1 day and amplitude $1/\Delta t_P$. (One day is very short compared to stratospheric transport time scales of years.) Furthermore, instead of using a two-dimensional tropopause mask $\Delta^{2d}(\mathbf{r}_\Omega, \Omega_i)$, we extend the mask in three dimensions through the troposphere. More precisely, during the pulse we replace $\Delta^{2d}(\mathbf{r}_\Omega, \Omega_i)$ with $\Delta^{3d}(\mathbf{r}, \Omega_i)$, which is unity everywhere below the tropopause if the latitude of $\mathbf{r}$ lies within the latitude bounds of Ω_i, and zero otherwise. The principal advantage of using this three-dimensional mask is that we avoid having to identify surface normals and instead need only build a mask that identifies grid points below Ω_i. In the limit of infinitesimal time step and pulse width the effect of applying this three-dimensional mask is equivalent to boundary condition (2).

[26] After the initial 1 day pulse we compute the mass flux per unit residence time, f, as the mass of tracer-labeled air that crosses into the troposphere, per time step δt, between successive application of the boundary condition. More precisely, if $\hat{\mathcal{G}}(\mathbf{r}, t_i + \tau|\Omega_i, t_i)$ denotes the tracer field $\mathcal{G}$ immediately before zeroing the troposphere, we compute $f(\Omega_f, t_i + \tau|\Omega_i, t_i)$ by integrating (with mass-weighted measure $\rho d^3 r$) $\hat{\mathcal{G}}(\mathbf{r}, t_i + \tau|\Omega_i, t_i)/(A(\Omega_f)\delta t)$ over the troposphere within the horizontal bounds of the final patch Ω_f (see also Appendix A). The exit patch Ω_f is typically chosen to be one of the Ω_i shown in Figure 2 or a longitudinal strip at latitude ϕ one grid box wide. This mask-budget approach is numerically robust, and has the enormous advantage of avoiding the explicit computation of the normal fluxes of $\mathcal{G}$ through the tropopause.

[27] Because of the long time scales of stratospheric transport, it takes several decades for $\mathcal{G}$ to decay from its peak value of $1/\Delta t_P$ at Ω_i to its ultimate value of zero everywhere. To capture the full evolution of $\mathcal{G}$, including the long-term asymptotic behavior, we integrate the model for 10,000 days and extrapolate the exponential tails for $\tau > 10{,}000$ days. The contributions from $\tau > 10{,}000$ days to integrals over all τ are evaluated analytically from the exponential extrapolation. The contributions from $\tau > 10{,}000$ days generally contribute less than 0.1% to the normalization of $\mathcal{G}$.

4. Results

[28] We present results derived from the ensemble averaged boundary propagator which, for our statistically stationary flow, depends on time only through $t - t_i$. We therefore drop all dependence on entry time t_i so that t denotes transit time since last tropopause contact. (Stratospheric residence time continues to be denoted by τ.) When Ω_f consists of a zonal strip a single grid box wide at latitude ϕ, we replace Ω_f with ϕ for notational convenience.

4.1. Evolution of $\mathcal{G}(\mathbf{r}, t|\Omega_{\mathrm{EQ}})$

[29] We begin by focusing on air entering the stratosphere at the tropical tropopause; that is, we focus on diagnostics based on $\mathcal{G}(\mathbf{r}, t|\Omega_i)$, with $\Omega_i = \Omega_{\mathrm{EQ}}$. Because the main pathway from anywhere in the troposphere into the upper stratosphere is through the tropical tropopause, the diagnostics for other Ω_i tend to be similar; any significant differences are noted below.

[30] Figure 3 shows the evolution of the ensemble-averaged, zonal mean boundary propagator $\mathcal{G}(\mathbf{r}, t|\Omega_{\mathrm{EQ}})$ with time t since last contact with Ω_{EQ}. Physically, $\mathcal{G}(\mathbf{r}, t|\Omega_{\mathrm{EQ}})\Delta t_P$ is the mass fraction of air at $(\mathbf{r}, t)$ that had a transit time in the interval $(t, t + \Delta t_P)$ since last contact with Ω_{EQ}. Note that $\mathcal{G}$ decays exponentially to its ultimate value of zero as all of the Ω_{EQ} air eventually returns back to the troposphere. For plotting purposes, in Figure 3, we have therefore normalized $\mathcal{G}(\mathbf{r}, t|\Omega_{\mathrm{EQ}})$ by its maximum value for each time t.

[31] The evolution of $\mathcal{G}$ is in accordance with our understanding of the stratospheric circulation. Air that enters the stratosphere at Ω_{EQ} undergoes diabatic upwelling in the tropics and isentropic quasi-horizontal transport into higher latitudes [e.g., *Holton et al.*, 1995; *Dethof et al.*, 2000;

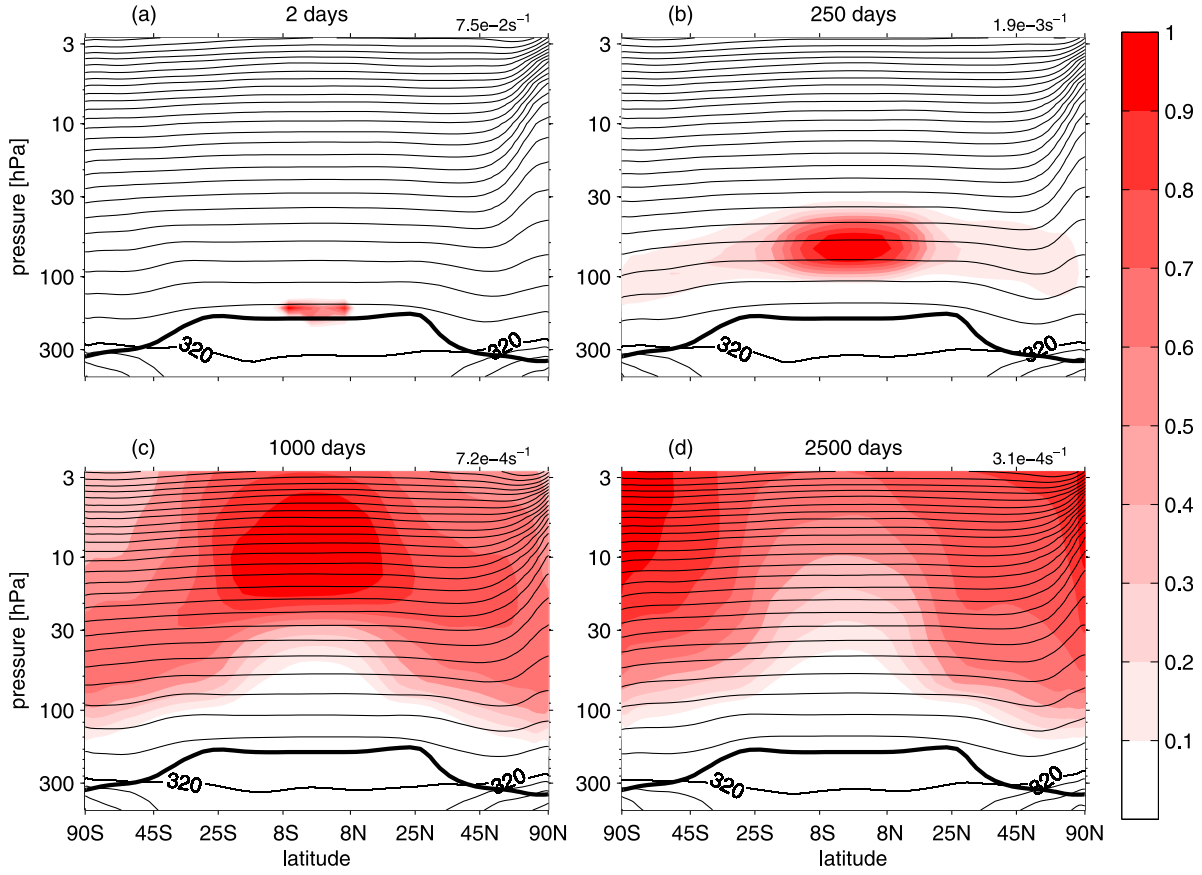

Figure 3. Colored field: the ensemble-averaged zonal mean boundary propagator, $\mathcal{G}(\mathbf{r}, t\,|\Omega_{EQ})$, after (a) 2, (b) 250, (c) 1000, and (d) 2500 days since last contact with the tropopause patch, Ω_{EQ}. Black contours: the time and zonal mean isentropes (10 and 40 K contour intervals for isentropes less than and greater than 320 K, respectively; the 320 K isentrope is labeled). Because $\mathcal{G} \to 0$ as $t \to \infty$, we normalize $\mathcal{G}(\mathbf{r}, t\,|\Omega_{EQ})$ for each value of t by its maximum indicated in the top right corner of each panel. The thick black line indicates the time and zonal mean thermal tropopause.

Plumb, 2002]. By day 250, Ω_{EQ} air is still upwelling through the tropical stratosphere with little vertical dispersion, and large-scale isentropic transport is also becoming evident. By day 1000 most of the Ω_{EQ} air has reached the upper stratosphere ($\sim$10 hPa) and spread significantly in both latitude and height.

[32] In less than $\sim$2500 days isopleths of Ω_{EQ} air have approached their characteristic poleward and downward sloping shapes. This corresponds to the "slope equilibrium" for long-lived constituents that results from the local balance between the slope-steepening effects of advection and the slope-flattening effects of eddy diffusion [*Plumb and Mahlman*, 1987; *Plumb and McConalogue*, 1988]. For $t >$ 2500 days, the mixing ratio of Ω_{EQ} air, $\mathcal{G}$, continuously decreases because of dilution and because of contact with the tropopause where the $\mathcal{G}$ label is removed by boundary condition (2). Fluctuations due to variability near the NH polar jet aside, isopleth shapes remain constant for $t >$ 2500 days.

4.2. The Flux Density Distribution $f(\phi, \tau|\Omega_{EQ})$

[33] The central quantity from which we derive all the diagnostic quantities of this study is the ensemble averaged flux density distribution $f(\phi, \tau|\Omega_i)$ shown in Figure 4 for $\Omega_i = \Omega_{EQ}$ as a function of stratospheric residence time τ and exit latitude ϕ. We first focus on the short-τ behavior and then discuss the overall structure of f.

[34] We emphasize that the expected short-τ singularity of f is a generic feature of the one-way flux if diffusive transport is present, regardless of the mechanism of the diffusion [*Hall and Holzer*, 2003]. Physically, the singular one-way flux arises from the quasi-random back-and-forth motion of fluid elements across the tropopause at the shortest resolved time and space scales. While our idealized GCM does not explicitly model subgrid-scale tracer transport with a diffusion term, tracers are nevertheless subject to numerical diffusion. Although it is most unlikely that this numerical diffusion is an accurate representation of the short time scale transport across the tropopause, the numerical diffusion may nevertheless be regarded as a model of such transport within the context of our highly idealized GCM. In that spirit, we examine the short-τ behavior of f to establish how the generic singular behavior manifests itself in our particular model.

[35] Figure 4 shows that $f(\phi, \tau|\Omega_{EQ})$ indeed exhibits nearly singular behavior as $\tau \to 0$ for latitudes $\phi \in \Omega_{EQ}$: in the tropics near the equator $f(\phi, \tau|\Omega_{EQ})$ is several orders of

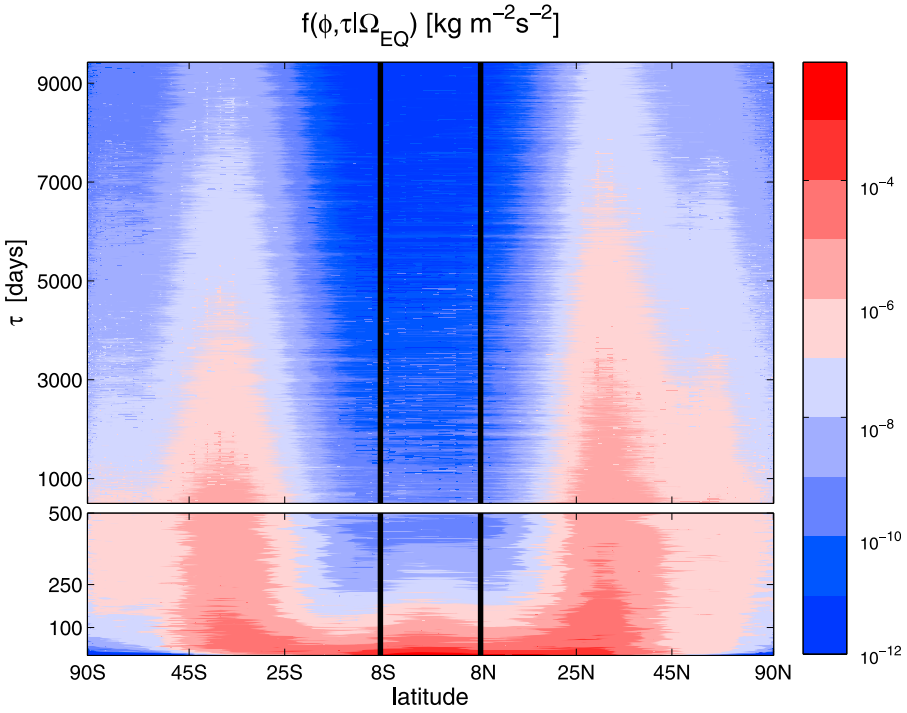

Figure 4. The ensemble and zonally averaged flux density of Ω_{EQ} air, $f(\phi, \tau|\Omega_{EQ})$. Note the logarithmic color scale, which is necessary to capture the full dynamic range of f, including the large fluxes at small residence times. The residence time axis is stretched for $\tau < 500$ days, so that the large short-τ fluxes and their rapid decay with τ are visible. The vertical lines mark the edges of Ω_{EQ}.

magnitude larger at $\tau = 3$ days than at $\tau \sim 30$ days (note that the color scale is logarithmic). The spatial discretization of the model keeps f finite even at $\tau = 0$; a true singularity is only expected in the continuum limit.

[36] In Figure 5 we quantify the functional form of the nearly singular short-τ behavior of f that is expected when $\Omega_f = \Omega_i$ by plotting $f(\Omega_i, \tau|\Omega_i)$ versus τ on a log-log plot. (Recall that $f(\Omega_i, \tau|\Omega_i)$ is the area average of $f(\phi, \tau|\Omega_i)$ over latitudes $\phi \in \Omega_i$.) Remarkably, for both $\Omega_i = \Omega_{EQ}$ and $\Omega_i = \Omega_{NM}$, f diverges approximately like $\tau^{-3/2}$ as $\tau \to 0$, as expected for Fickian diffusion, in spite of the fact that our model contains only numerical diffusion. Although there is significant ensemble variability, the divergence appears to be sharper and closer to a $\tau^{-3/2}$ power law for the case $\Omega_i = \Omega_{NM}$ than for the case $\Omega_i = \Omega_{EQ}$. It is unclear why at midlatitudes there appears to be a slightly stronger "Fickian divergence," but it may be related to the sharper vertical gradients of $\mathcal{G}$ produced by the downwelling branch of the BDC, which keeps labeled air closer to the tropopause.

[37] We now return to Figure 4 and examine the structure of the flux density distribution away from the singularity. As seen in Figure 4, between ~20°S and ~20°N the flux density rapidly decreases with increasing τ, decaying to less than 5% of its value at 5 days in about one month. This may be due to the presence of a tropical barrier to horizontal transport that prevents the return flow of Ω_{EQ} air back into the tropical tropopause following upwelling and spreading to higher latitudes. This barrier is manifest by the sharp spatial gradients of the flux density around 20°S/N that move slightly poleward and attenuate with increasing τ. Observed stratospheric trace gases feature similar gradients suggesting a tropical barrier to horizontal mixing with important implications for stratospheric chemistry [*Plumb*, 1996].

[38] The pattern of $f(\phi, \tau|\Omega_{EQ})$ is strikingly different at midlatitudes than in the tropics. The return flux across the midlatitude tropopause is composed of air that, at different stages during upwelling out of the tropics, crosses the tropical barrier isentropically and spends a broad range of times recirculating in the extratropical stratosphere before descending back into the troposphere. The large short-τ fluxes of Ω_{EQ} air at midlatitudes are most likely due to rapid isentropic transport. They cannot be due to rapid diffusively dominated return fluxes because the midlatitudes do not overlap with Ω_{EQ}.

[39] The dominant feature of the flux pattern seen in Figure 4, aside from the large fluxes at short τ, is the midlatitude ridge in each hemisphere between ~20° and ~45°. These ridges represent the adiabatic conduits into the troposphere provided by the 320–350 K isentropes that cut across the tropopause. The midlatitude flux is seen to be fed by air with a wide range of stratospheric residence times: It takes ~8000 days for the midlatitude flux to decay to the levels reached in a mere 250 days in the tropics.

[40] An intriguing feature of the flux pattern of Figure 4 is that midlatitude fluxes persist longer in the NH where, because of perpetual DJF conditions and midlatitude topography, the BDC is stronger. This may be due in part to the NH air drifting along streamlines of the Brewer-Dobson residual mean circulation that extend much higher in the NH than in the SH due to the asymmetric topographic distribution and temperature relaxation in the model.

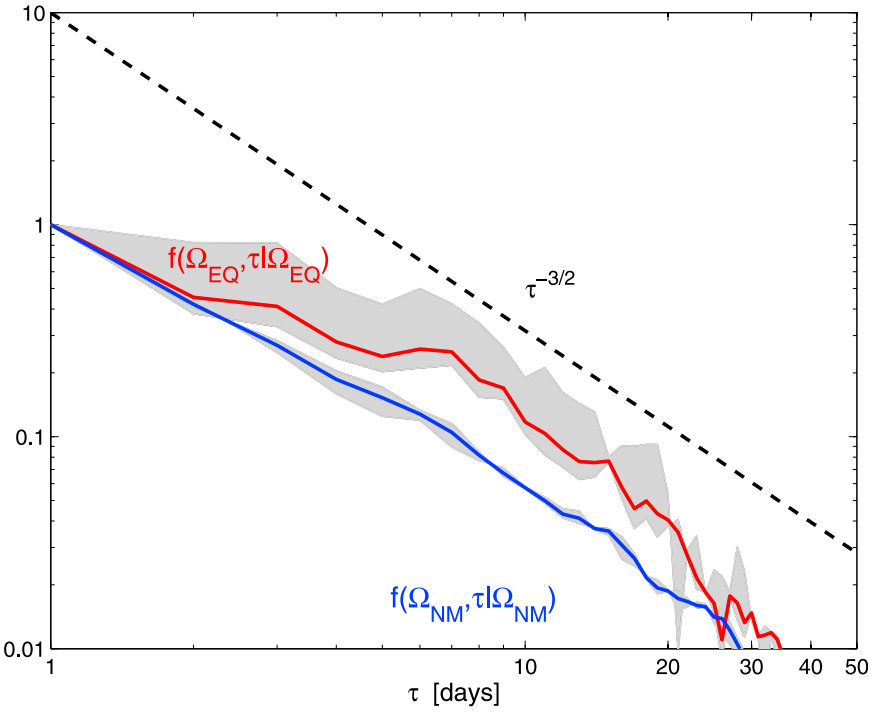

Figure 5. The ensemble-averaged flux density per unit residence time, $f(\Omega_i, \tau|\Omega_i)$, for overlapping entry and exit patches ($\Omega_f = \Omega_i$) for $\tau < 50$ days. For plotting, $f(\Omega_i, \tau|\Omega_i)$ has been normalized by its value for $\tau =$ 1 day. Two cases are shown: $\Omega_i = \Omega_{NM}$ (blue line) and $\Omega_i = \Omega_{EQ}$ (red line). Grey shading indicates one standard deviation of the ensemble spread. The dashed line indicates a $\tau^{-3/2}$ power law to guide the eye.

[41] Consistent with the fact that f extends to longer residence times in the NH, we find that the mass of EQ air is at all times larger in the NH than in the SH. Thus, air labeled symmetrically about the equator is transported preferentially into the NH upon entry into the stratosphere. This, along with increased recirculations in the NH associated with strong wave breaking and stratospheric sudden warming events (in contrast to the more quiescent SH stratosphere), all appear to conspire to increase the amount of long–residence time ("old") air exiting through the NH midlatitudes. We quantify the hemispheric asymmetry more precisely below in section 4.4.2 in terms of the mean residence time $\bar{\tau}$.

[42] So far we discussed the flux density for the particular case of Ω_{EQ} air. For other entry patches Ω_i, the flux distributions differ most noticeably at short residence times for latitudes within Ω_i, where the distributions are nearly singular. The degree of hemispheric asymmetry in the flux density pattern also depends on Ω_i, with air entering the stratosphere at either polar patch only moving negligibly into the opposite hemisphere. At large residence times ($\tau > 4000$ days), however, the flux patterns become independent of Ω_i as one would expect because mixing, when acting for a long time, erases any memory of entry region.

4.3. The Cumulative Mass Flux $\mathcal{F}(\phi, \tau^*|\Omega_{EQ})$

[43] We now ask what is the one-way flux of air that has had residence times longer than a specified threshold τ^*. To this end we compute the cumulative mass flux $\mathcal{F}(\phi, \tau^*|\Omega_i) \equiv \int_{\tau^*}^{\infty} d\tau f(\phi, \tau|\Omega_i)$. The cumulative flux is relevant, for example, if we wish to quantify the importance of very old air.

[44] Figure 6 shows $\mathcal{F}(\phi, \tau^*|\Omega_i)$ for $\tau^* = 300$ and 3000 days (in red and blue, respectively), and for $\Omega_i = \Omega_{SM}$, Ω_{EQ}, and Ω_{NM}. Note that by excluding residence times shorter than a finite τ^*, $\mathcal{F}(\phi, \tau^*|\Omega_i)$ is finite even for latitudes $\phi \in \Omega_i$. Interestingly, for $\Omega_i = \Omega_{EQ}$, the flux of air with $\tau > \tau^*$ returning through latitudes $\phi \in \Omega_{EQ}$ is negligible compared to the return flux through the entry patch for the other cases. This is true even for τ^* less than one month (not shown), emphasizing that the only significant return flow back through the tropical tropopause is associated with very short-τ eddy-diffusive processes. By contrast, for $\Omega_i = \Omega_{SM}$ or Ω_{NM} there is a significant flux back through the entry patch even for finite τ^*.

[45] The pronounced peaks of $\mathcal{F}$ at midlatitudes seen in Figure 6 again highlight the fact that the primary S → T conduit is isentropic transport [e.g., *Chen*, 1995; *Dethof et al.*, 2000]. The cumulative flux of Ω_{EQ} air with $\tau^* =$ 300 days also quantifies pronounced interhemispheric asymmetry with 2.5 times larger flux into the NH than into the SH. The cumulative flux for $\tau^* = 3000$ days shows that the S → T flux of old air takes place predominantly at midlatitudes (64% passes through Ω_{NM} and 15% through Ω_{SM}).

4.4. The $\Omega_i \rightarrow \Omega_f$ Mass Fraction and Mean Residence Time

4.4.1. Mass Fraction $\mu(\Omega_i, \Omega_f)$

[46] The residence time partitioned mass fraction of the stratosphere $\mathcal{R}(\tau, \Omega_i, \Omega_f) \propto \tau f(\Omega_f, \tau|\Omega_i)$, discussed in section 2, contains key transport information that we now summarize in terms of its moments $\mu(\Omega_i, \Omega_f)$ and $\bar{\tau}(\Omega_i, \Omega_f)$.

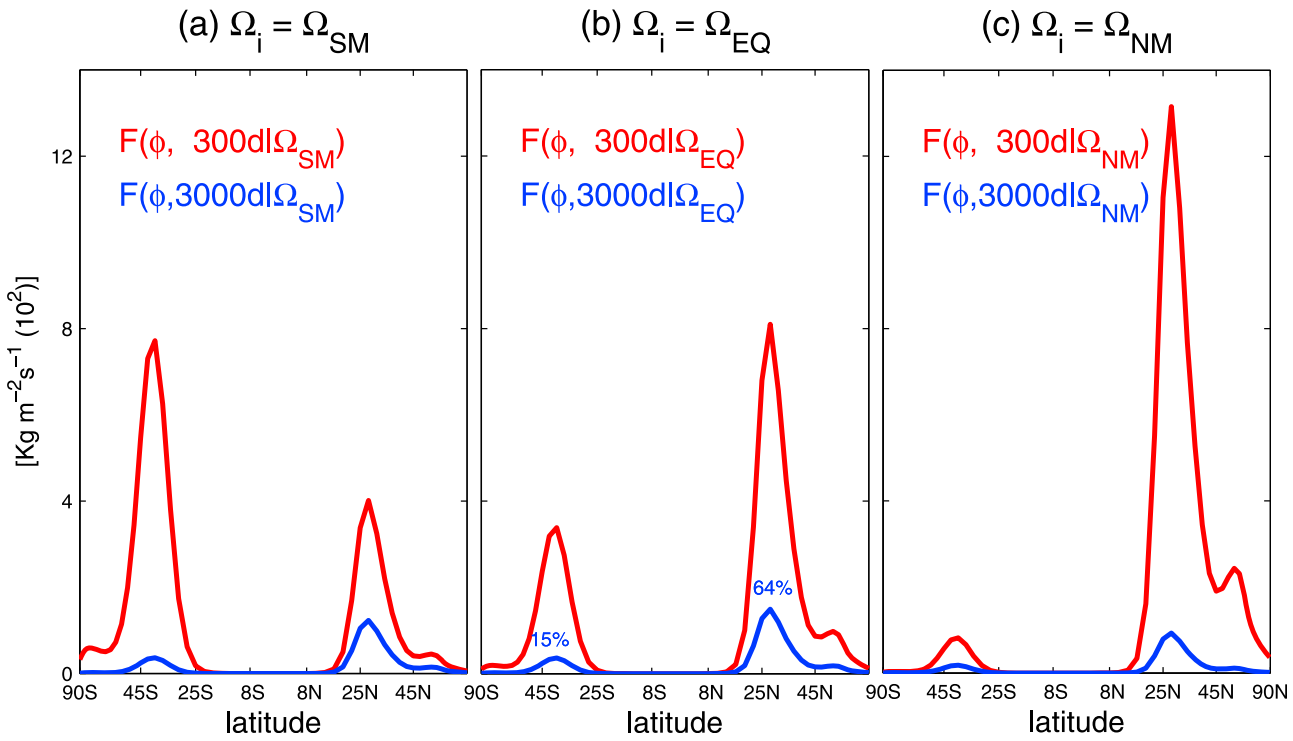

Figure 6. The ensemble and zonally averaged cumulative flux of air, $\mathcal{F}(\phi, \tau^*|\Omega_i)$ for τ^* = 300 days (red line) and 3000 days (blue line) for (a) $\Omega_i = \Omega_{SM}$, (b) $\Omega_i = \Omega_{EQ}$, and (c) $\Omega_i = \Omega_{NM}$. The percentages in Figure 6b indicate the fraction of the globally integrated $\mathcal{F}(\phi, \tau^*|\Omega_i)$ that leaves through Ω_{SM} and Ω_{NM} for τ^* = 3000 days.

These quantities were computed from the ensemble averaged flux density using (4), (6), and (7).

[47] Figure 7 shows $\mu(\Omega_i, \phi)$, the mass fraction of the stratosphere in transit from Ω_i to longitudinal grid strip at latitude ϕ, for each of our seven Ω_i patches (Figures 7a–7c). Figure 7d also shows $\mu(\Omega, \phi)$, the mass fraction that exits at ϕ regardless of where the air entered ($\Omega_i = \Omega$). Note that the mass fractions plotted in Figure 7 are normalized so that $\Sigma_{f=1}^{64}\Sigma_{i=1}^{7}\mu(\Omega_i, \phi_f) = 1$ (our model grid has 64 latitudes).

[48] The key result shown in Figure 7 is that the largest mass fractions of the stratosphere return to the troposphere primarily (1) through where the air entered (Ω_i) and (2) through the isentropic midlatitude conduits, with a larger fraction of the stratosphere destined to NH exit latitudes than to SH exit latitudes. Furthermore, $\mu(\Omega_i, \phi)$ quantifies exactly how much of the stratosphere is destined for each exit latitude ϕ, given that it entered through a specified Ω_i. Thus, for example, Ω_{SM} and Ω_{ST} air destined for the NH midlatitudes constitute similar fractions of the total stratospheric mass (9.1% and 16.9% respectively, as indicated in Figure 7b), suggesting similar paths into the NH. Preferential exit through the NH midlatitudes compared to the SH midlatitudes is clearly evident for Ω_{EQ} air (Figure 7c), and for all air regardless of entry location (Figure 7d).

[49] The large fractions of the stratosphere that are in transit back to the regions where they entered from the troposphere are visible in Figure 7 as the dominant peaks in $\mu(\Omega_i, \phi)$ for $\phi \in \Omega_i$. These peaks can be attributed to the short-τ diffusive singularity. Excluding residence times less than a few days in the calculation of μ (not shown) eliminates the peaks in $\mu(\Omega_i, \phi)$ for latitudes $\phi \in \Omega_i$. Interestingly, the stratospheric mass fraction including all possible entry locations, $\mu(\Omega, \phi)$ (Figure 7d), remains largest for midlatitude exit. This shows that the short-τ near-singular return flux does not carry enough mass to overwhelm the contribution from air with longer residence times leaving through the isentropic midlatitude conduits across the tropopause.

4.4.2. The Mean Residence Time $\bar{\tau}$

[50] Stratospheric air has a broad distribution of residence times, which for given Ω_i and Ω_f is given by $\mathcal{R}(\tau, \Omega_i, \Omega_f)/\mu(\Omega_i, \Omega_f)$. A convenient summary of this distribution is provided by its first moment $\bar{\tau}(\Omega_i, \Omega_f)$, the mean residence time of Ω_i air that leaves the stratosphere through Ω_f, defined in equation 7.

[51] Consider first $\bar{\tau}(\Omega_{EQ}, \phi)$, plotted in Figure 8a. For latitudes $\phi \in \Omega_{EQ}$, $\bar{\tau}$ is very small (~5 days), which reflects the overwhelming importance of the diffusive return flux through Ω_{EQ} of air with very short residence times. From the edges of Ω_{EQ} to latitude ±~30°, $\bar{\tau}$ increases to ~2500 days in the SH and to ~3000 days in the NH. The fact that mean residence times are longer in the NH than in the SH, as anticipated from the structure of $f(\phi, \tau|\Omega_i)$, is by no means a trivial result: a stronger NH BDC might naively be expected to lead to more vigorous flushing and hence shorter NH residence times as compared to the SH. However, in the NH the higher-reaching paths and increased eddy diffusion win out over the stronger advection by the residual mean stream function. (By eddy diffusion we mean the quasi-random transport due to breaking Rossby waves [e.g., *Holton et al.*, 1995; *Plumb*, 2002; *Kazuyuki et al.*, 2010]). The net effect is a longer $\bar{\tau}$ in the NH, where the BDC is stronger. This underlines the fact that the BDC captures only advection by

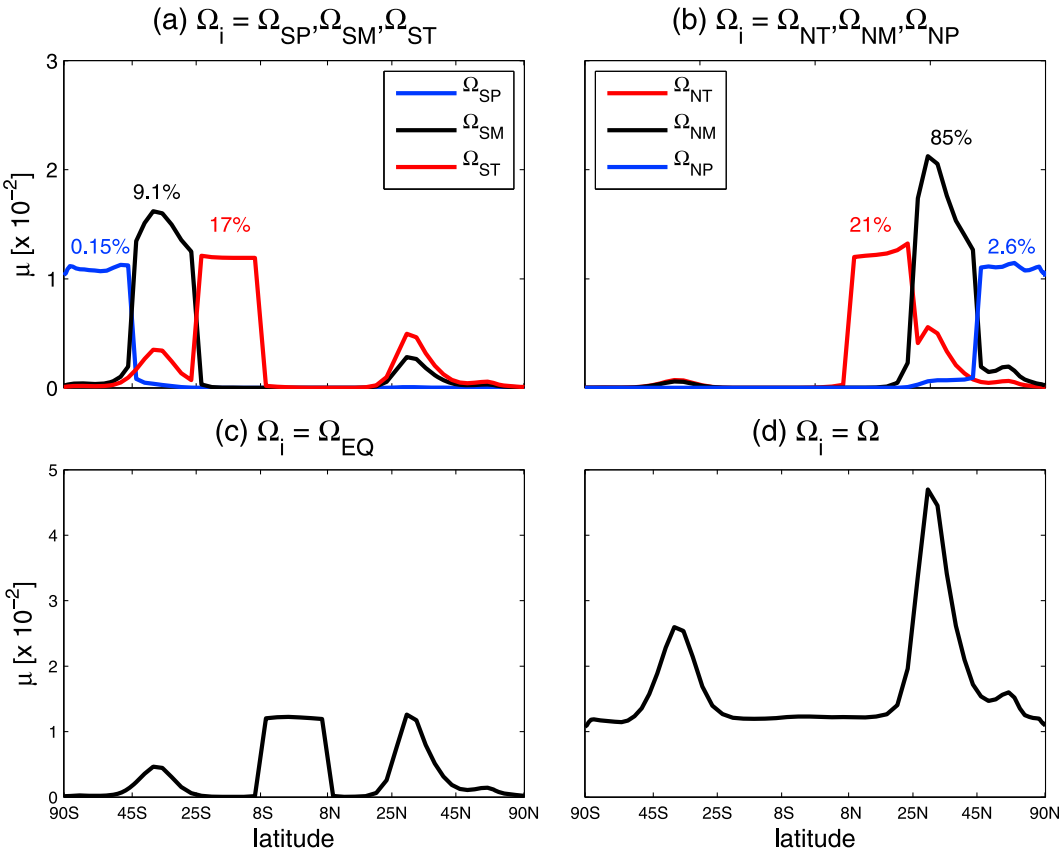

Figure 7. The ensemble-averaged mass fraction $\mu(\Omega_i, \phi)$ of the stratosphere that undergoes $\Omega_i \rightarrow \phi$ transport for Ω_i in (a) the Southern Hemisphere, (b) the Northern Hemisphere, (c) $\Omega_i = \Omega_{EQ}$, and (d) the full tropopause, $\Omega_i = \Omega$. In Figures 7a and 7b the percentage of the total stratospheric mass undergoing $\Omega_i \rightarrow \Omega_{NM}$ transport is indicated for the color-coded Ω_i cases shown.

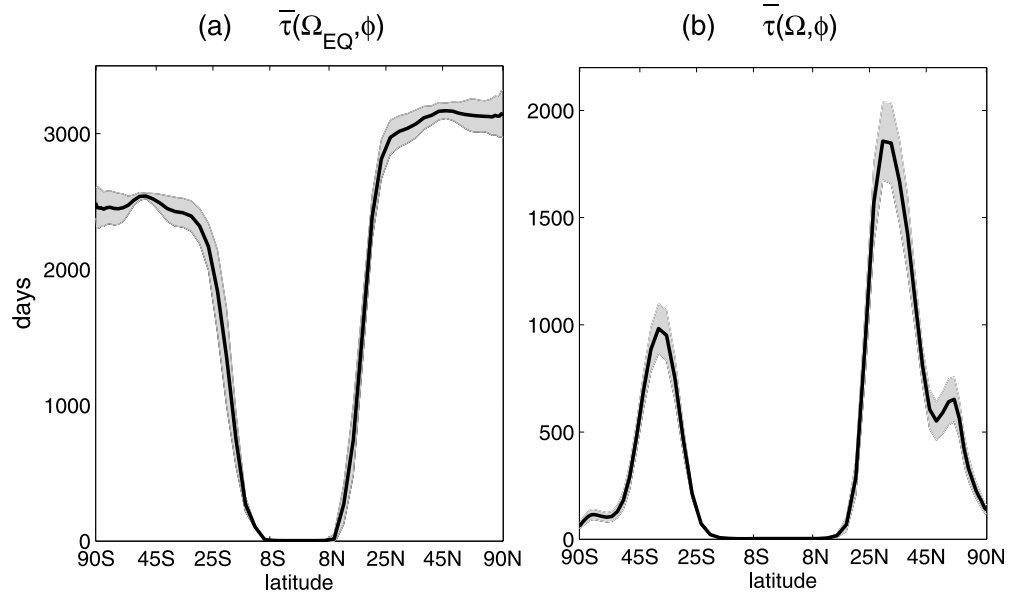

Figure 8. (a) The mean residence time, $\bar{\tau}(\Omega_{EQ}, \phi)$, of Ω_{EQ} air exiting the stratosphere at latitude ϕ. The thick line indicates the ensemble average, and the grey shading indicates one standard deviation of the ensemble spread. (b) The mean residence time, $\bar{\tau}(\Omega, \phi)$, of air regardless of where it entered.

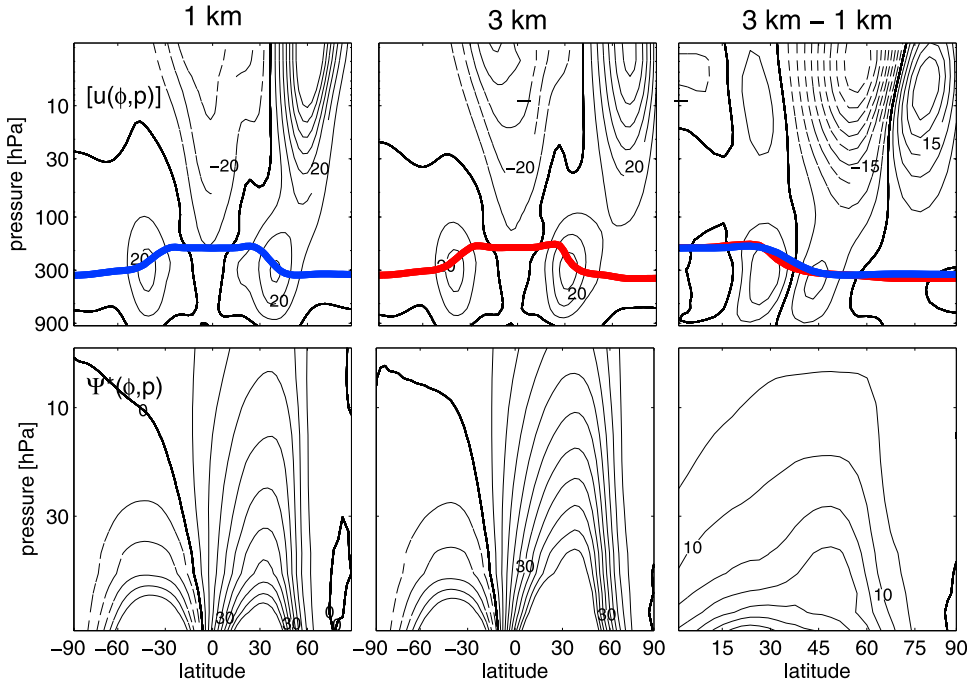

Figure 9. (top) The ensemble and zonally averaged zonal winds [u] and (bottom) residual mean stream function Ψ^* for topography amplitudes of (left) 1 km, (middle) 3 km, and (right) their $\Delta_{3km-1km}$ differences. Note that the difference fields are shown only for the Northern Hemisphere, where the circulation changes are most pronounced. The contour spacing for [u] is 10 m s^{-1} (Figures 9 (left) and 9 (middle)) and 5 m s^{-1} (Figure 9 (right)); the zero-wind contour is bold, and easterly winds are dashed. Stream function contours are spaced 15 kg m^{-1} s^{-1} apart; the zero line is bold, and negative streamlines are dashed. The time and zonal mean thermal tropopause is indicated in Figure 9 (top) in blue (1 km) and red (3 km).

the residual mean drift through the stratosphere and not the effects of quasi-horizontal eddy diffusion, which is also stronger where the wave forcing is stronger.

[52] Poleward of ∼30° in both hemispheres, $\bar{\tau}(\Omega_{EQ}, \phi)$ is essentially constant all the way to the poles. While much more Ω_{EQ} air leaves at midlatitudes than at the poles (Figures 4 and 6), rapid isentropic mixing appears to ensure that air exiting at any latitude poleward of 30° has a residence time distribution of similar shape. Consequently, $\bar{\tau}$ is nearly constant poleward of ∼30°.

[53] Figure 8b shows $\bar{\tau}(\Omega, \phi)$, the mean residence time of air that exits at latitude ϕ regardless of where it entered ($\Omega_i = \Omega$). The short-τ eddy diffusive $\phi \rightarrow \phi$ return flux dominates nearly the entire tropics to the degree that $\bar{\tau}$ is nearly zero there and dramatically reduces $\bar{\tau}(\Omega, \phi)$ at high latitudes compared with $\bar{\tau}(\Omega_{EQ}, \phi)$. At midlatitudes $\bar{\tau}(\Omega, \phi)$ is also reduced compared with $\bar{\tau}(\Omega_{EQ}, \phi)$ but only by a factor of roughly two. This attests to the substantial flow of old air out of midlatitudes so that mean residence time does not become overwhelmed by short-τ eddy transport, as is the case for the tropics.

5. Changes in STE in Response to Idealized Circulation Changes

[54] We now ask how the flux distributions and the residence time partitioning of the mass of the stratosphere respond to changes in the circulation. Capitalizing on the idealized nature of our model, a natural choice for inducing circulation changes is to change the amplitude of the NH midlatitude topography. We therefore compute an additional five-member ensemble with the topography amplitude reduced from 3 km to 1 km, keeping all other parameters unchanged. The decreased topography reduces the flux of planetary waves into the polar vortex; less wave drag in the middle stratosphere results in a weaker residual mean circulation.

5.1. Response of Residual Mean Flow to Changes in Topography

[55] Figure 9 summarizes the circulation changes. Differences are calculated with respect to the 1 km ensemble, that is, for quantity X we define $\Delta X \equiv X_{3km} - X_{1km}$. The changes in the zonal mean zonal wind (Figure 9, top) show that the NH polar vortex is weaker and further poleward with higher topography because more planetary waves propagate up from the troposphere and break in the stratosphere, depositing westward momentum and decelerating the vortex. In response, the tropospheric midlatitude jet shifts equatorward (∼40°N → 32°N) [see also, e.g., *Polvani and Kushner*, 2002; *Gerber and Polvani*, 2009]. Correspondingly, the NH high-gradient region of the tropopause height shifts equatorward with increased wave forcing.

[56] Figure 9 (bottom) shows the changes in the time and ensemble mean mass stream function Ψ^* of the residual mean circulation [*Andrews et al.*, 1987]. With higher topography the BDC strengthens throughout the NH and reaches higher into the NH stratosphere. We note in passing

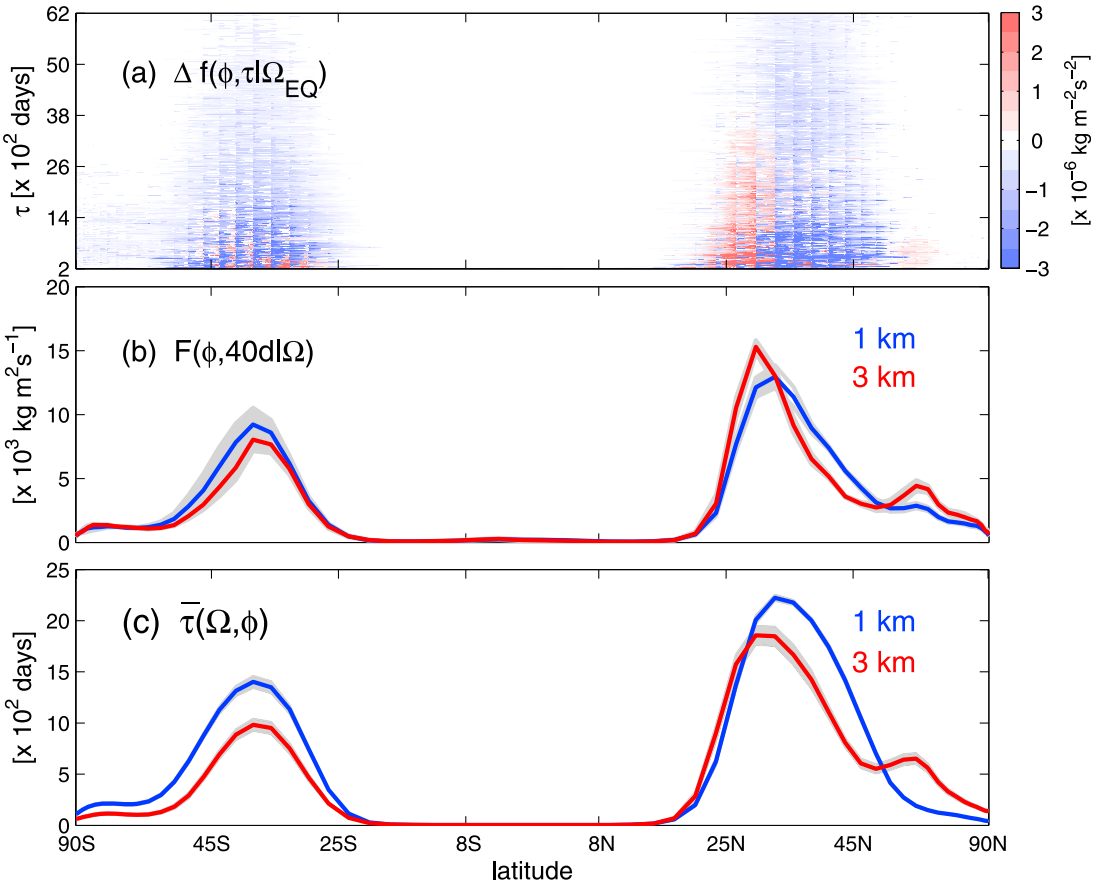

Figure 10. (a) The difference between the 3 and 1 km ensemble and zonally averaged flux density, $\Delta f(\phi, \tau|\Omega_{EQ})$. Note that the τ axis only extends from 200 to 6200 days so that the fluxes can be plotted with a linear color scale.(b) The ensemble averaged cumulative flux $\mathcal{F}(\phi, 40d|\Omega)$, which is the flux of air exiting at latitude ϕ that has resided in the stratosphere for 40 days or longer, regardless of where it entered ($\Omega_i = \Omega$). The ensemble mean fluxes are shown in blue for the 1 km case and in red for the 3 km case. Grey shading indicates the standard error of the ensemble mean. (c) The mean residence time of air entering anywhere at the tropopause, $\bar{\tau}(\Omega, \phi)$, for the 1 (blue) and 3 km (red) topography cases along with the associated standard error (grey shading).

that the strengthening of Ψ^* is similar to the climate change response of the BDC simulated with comprehensive chemistry climate models by *McLandress and Shepherd* [2009].

5.2. Response of STE to Circulation Changes

5.2.1. Changes in the Flux Distribution

[57] Figure 10a shows the ensemble mean change $\Delta f(\phi, \tau|\Omega_{EQ})$ of the flux density distribution of Ω_{EQ} air as a function of ϕ and τ. The strengthened BDC in the NH leads to an increased S →T flux of Ω_{EQ} air at high northern latitudes for all residence times. The equatorward shift of the cross-tropopause isentropic conduits manifests itself as a spatially dipolar pattern in Δf at subtropical and midlatitudes that is pronounced in the NH. Note that this 'dipole' is skewed toward negative values indicating an overall weakening of the midlatitude fluxes.

[58] The changes in the one-way S → T flux are more easily quantified in terms of the cumulative flux $\mathcal{F}$. To account for all possible transport pathways, we consider $\Omega_i = \Omega$, that is, the flux of air regardless of where it entered the stratosphere. Figure 10b shows $\mathcal{F}(\phi, \tau^*|\Omega)$ for $\tau^* = 40$ days to capture the changes in the S → T flux away from the nearly singular short-τ regime. In the NH, the stronger BDC (3 km topography) leads to an increase of ~20% in the peak midlatitude flux and of ~30% in the secondary peak at high latitudes. Between these peaks $\mathcal{F}(\phi, 40d|\Omega)$ decreases significantly, consistent with the "skewed dipole" of Δf in Figure 10a. In the SH, the cumulative fluxes decrease slightly. The changes in the flux distributions have important consequences for the stratospheric mean residence time $\bar{\tau}$, which we examine next.

5.2.2. Changes in Mean Residence Time

[59] Changes in $\bar{\tau}$ have implications for chemical composition because $\bar{\tau}$ provides a scale for chemical lifetimes. Chemical species with lifetimes longer than $\bar{\tau}$ are likely to survive their passage through the stratosphere and can hence reenter and influence the troposphere, while species with lifetimes shorter than $\bar{\tau}$ are likely to react within the stratosphere.

[60] Figure 10c shows $\bar{\tau}(\Omega, \phi)$, the mean residence time of air exiting at latitude ϕ regardless of where it entered ($\Omega_i = \Omega$), for both the 1 and 3 km ensembles. With a

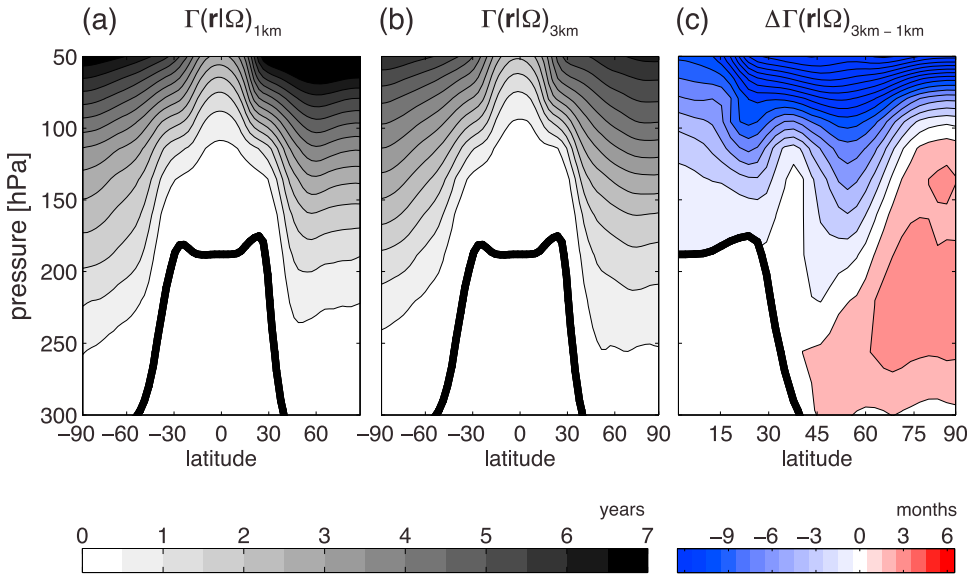

Figure 11. The ensemble-averaged mean age $\Gamma(\mathbf{r}|\Omega)$ of air entering the stratosphere anywhere at the tropopause for the (a) 1 and (b) 3 km topography cases. (c) The difference $\Delta\Gamma(\mathbf{r}|\Omega)$ between the ensembles for the Northern Hemisphere, where the circulation changes are most pronounced. The contour interval is 6 months for Γ and 2 months for $\Delta\Gamma$, straddling $\Delta\Gamma = 0$ symmetrically. The time and zonal mean thermal tropopause for the 3 km ensemble is indicated as a thick black line.

stronger BDC, $\bar{\tau}(\Omega, \phi)$ decreases by ~300 days at midlatitudes in both hemispheres but increases by ~500 days at high latitudes in the NH. The decrease at NH midlatitudes is what one might expect from a faster NH BDC if the changes in circulation are advectively dominated. The decrease in the SH, where the BDC hardly changes, may be due to the following mechanism: With a stronger NH BDC (3 km topography), air upwelling in the tropical stratosphere will be preferentially transported to the NH (see also section 4.2). This may divert air that would otherwise travel via the slower SH pathways through the upper stratosphere thereby decreasing the mean residence time of air exiting in the SH.

[61] A particularly interesting result is the substantial increase in $\bar{\tau}(\Omega, \phi)$ at high NH latitudes. That $\bar{\tau}$ would increase anywhere because of a stronger stratospheric circulation is not a priori obvious. The increase in $\bar{\tau}$ points to the fact that a stronger circulation (3 km topography) also has higher-reaching, longer paths to Arctic latitudes and stronger eddy-diffusive transport that is not captured by the residual mean stream function, Ψ^* [see also *Holzer*, 2009b]. Increased $\bar{\tau}$ for air exiting poleward of 50°N suggests that in a future climate with a stronger BDC there will be an increased S → T flux of long-lived (and a decreased flux of short-lived) chemical species into the Arctic troposphere. We note that the flux out of the stratosphere north of 50°N accounts for 10% of the total S → T flux for air that entered anywhere and has $\tau > 3000$ days.

[62] While mean residence time cannot be deduced from mean age, robust changes in the two diagnostics must be mutually consistent. That this is the case is confirmed by Figure 11, which compares the ensemble averaged mean age of air, $\Gamma(\mathbf{r}|\Omega)$, since last contact anywhere on the tropopause for the two topography cases. The mean age $\Gamma(\mathbf{r}|\Omega)$ is computed as the first moment of the ensemble averaged $\mathcal{G}(\mathbf{r}, \tau|\Omega)$, normalized so that $\int_0^\infty \mathcal{G}(\mathbf{r}, \tau|\Omega)d\tau = 1$. As expected, $\Delta\Gamma$ shows that Γ decreases in most places in response to a stronger BDC. However, consistent with the increase in $\bar{\tau}(\Omega, \phi)$ over NH high latitudes, $\Delta\Gamma(\mathbf{r}, \Omega)$ shows an increase of ~0.5 years in the lower stratosphere at these latitudes. Thus, longer mean residence times for air exiting poleward of 50°N are not only associated with slower returns to the tropopause, but also with slower paths from the tropopause into the lower stratosphere.

6. Summary and Conclusions

[63] We have presented the first well defined one-way flux diagnostics of STE. At the center of our analyses is the flux density distribution, $f(\Omega_f, \tau|\Omega_i)$, that partitions the one-way, or "gross," cross-tropopause mass flux with respect to residence time τ in the stratosphere, entry region Ω_i, and exit region Ω_f. The flux density distribution robustly captures the $\Omega_i \rightarrow \Omega_f$ flow through the stratosphere without being rendered ill defined by the short-τ eddy-diffusive singularity for overlapping Ω_i and Ω_f; the diffusive singularity merely imparts short-τ structure to the distribution. In addition to quantifying the one-way flux, suitable integrations of the flux density yield the ensemble averaged mean residence time in the stratosphere, $\bar{\tau}(\Omega_i, \Omega_f)$, and the ensemble averaged mass fraction $\mu(\Omega_i, \Omega_f)$ of the stratosphere undergoing $\Omega_i \rightarrow \Omega_f$ transport. To the best of our knowledge, this is the first application of these diagnostics to STE and the first calculation of the one-way flux distribution for transport across a time-evolving surface.

[64] We emphasize that the main point of this paper has been to illustrate a new tracer-independent diagnostic of stratospheric transport. Our flux distributions do not represent the flux of any particular chemical species, but instead quantify the one-way flux of air binned with respect to τ, Ω_i,

and Ω_f. The flux distributions and the underlying boundary propagators can be convolved with boundary conditions at the tropopause for particular species and weighted with decay functions of the time spent in the stratosphere to model particular chemical species. In this way our diagnostics can be used to isolate the role of transport from that of chemistry, but the analysis of specific tracers is beyond the scope of this paper.

[65] In the interpretation of our results it must firmly be kept in mind that the model's semi-Lagrangian advection numerics were only corrected for global conservation and are therefore subject to local flux errors. For the purpose of illustrating our new STE diagnostics, we accept the limitations of an idealized atmosphere and semi-Lagrangian numerics. A better, strictly conservative scheme may well result in solutions that differ in detail from ours, but we believe that the semi-Lagrangian scheme suffices to capture the qualitative features of STE revealed by our diagnostic. We stress that for any given numerical transport scheme the numerical implementation of our flux diagnostics is robust because it avoids the need for flux vectors and surface normals.

[66] We remind the reader that our model was run under perpetual DJF conditions with topography only in the NH. The resulting idealized flow has a hemispherically asymmetric BDC that is stronger in the NH. Our main findings are as follows:

[67] 1. The latitudinal structure of the flux density of tropical air, $f(\phi, \tau|\Omega_{EQ})$, reveals several key features of STE. The flow of Ω_{EQ} air back through equatorial patch Ω_{EQ} is dominated by short-τ diffusive fluxes that rapidly decay with increasing τ because a barrier to horizontal transport prevents a return to the tropics following upwelling and spreading to higher latitudes. For $\tau \sim 200$ days, the dominant feature of $f(\phi, \tau|\Omega_{EQ})$ is persistent fluxes at midlatitudes where isentropes cross the tropopause. These midlatitude fluxes of Ω_{EQ} air capture paths with a wide distribution of residence times and exhibit strong hemispheric asymmetry particularly for old air.

[68] 2. Analysis of $\mu(\Omega_i, \phi)$, the ensemble averaged mass fraction of the stratosphere in transit from Ω_i to exit at latitude ϕ, shows that most of the stratospheric air mass returns to the troposphere via two pathways: (1) air recrosses the tropopause where it entered and (2) air crosses the tropopause isentropically at midlatitudes. While a substantial fraction of the stratosphere returns through the short-τ dominated $\Omega_i \rightarrow \Omega_i$ "short circuits", the largest mass fraction of the stratosphere regardless of entry location returns through midlatitudes with a broad range of residence times. The short-τ near-singular return flux does not carry enough mass to overwhelm the contribution from air with longer residence times that leaves isentropically at midlatitudes.

[69] 3. An intriguing result from the idealized model is that the mean residence time $\bar{\tau}$ of air exiting through the NH is longer than the mean residence time of air exiting through corresponding SH latitudes. For exit at midlatitudes, $\bar{\tau}$ is nearly twice as large in the NH. This was certainly not a priori obvious given that the stronger NH BDC circulation might be expected to flush the NH stratosphere more efficiently. However, a higher-reaching residual mean stream function, a more turbulent, eddy-diffusive stratosphere with more breaking Rossby waves, and more frequent sudden stratospheric warmings, all combine to lengthen the advective-diffusive paths through the NH stratosphere. Remarkably, compared to the SH, these effects win out over faster advection by the residual mean stream function.

[70] 4. We quantified how STE changes in response to changes in the circulation induced by varying the amplitude of the idealized NH topography. The mean residence time of air, regardless of where it entered the stratosphere, is reduced when the topography is increased by ~300 days for exit at midlatitudes in either hemisphere, while the mean residence time for exit at high NH latitudes increases by ~500 days. Consistently, the mean age decreases throughout the stratosphere, except in the lowermost NH stratosphere where it increases by ~0.5 years.

[71] Comparing the effect of increased topographic wave forcing between the hemispheres and between the 1 and 3 km amplitude ensembles shows that the control of topographic forcing on tropopause-to-tropopause transport is subtle and involves competing mechanisms. Compared to no topography at all, the stronger residual mean circulation with topographically forced waves is dominated by increased eddy-diffusive recirculations and longer effective paths. As a result NH one-way fluxes persist over longer residence times than their SH counter parts with correspondingly longer mean residence times. However, when increasing the topography amplitude from 1 to 3 km, the resulting stronger wave driving is less successful at further enhancing eddy diffusion and the faster residual mean circulation leads to reduced mean residence times except for air exiting at high latitudes in the NH, where lengthened paths and increased eddy diffusion further increase mean residence time. The fact that competing mechanisms control the integrated advective-eddy-diffusive transport through the troposphere underlines the fact that advection by the residual mean stream function cannot fully capture tropopause-to-tropopause transport.

[72] While beyond the scope of the current study, more systematic investigations of the dependence of stratospheric mean residence times on the amplitude of forced waves and analytical modeling of simplified stratospheric circulations are needed for a detailed understanding of how these waves, and more generally the competition between diffusion and advection, control STE.

[73] Our analysis exploits simplifications afforded by the stationarity of the ensemble mean flow. For time-varying flows, computation of the mass of the stratosphere at a given time that will ultimately have a specified residence time would require many tracers. However, for time-varying, nonensemble averaged flow it is natural to partition not the entire mass of the stratosphere, but only the mass of the air that enters through a specified entry patch Ω_i during a specified time interval. The partitioning of this Ω_i air mass according to residence time and exit location can be computed from its flux density distribution as was done here, except that the mass and time integral of the boundary propagator for Ω_i air must be explicitly normalized a posteriori (for details, see *Holzer* [2009a, 2009b]).

[74] Finally, we emphasize that the diagnostics explored in this paper in the context of an idealized model are straightforward to compute within any circulation model capable of carrying conservative tracers. The flux density distribution, and the diagnostics derivable from it, are a natural way to

quantify STE, and we plan to apply this methodology to comprehensive circulation models.

Appendix A: Algorithm to Compute Mass Flux Density f

[75] To compute the one-way S → T flux across the tropopause at time t of air that entered the stratosphere at Ω_i during the time interval $(t_i, t_i + \Delta t_P)$, perform the following steps at every model time t.

[76] 1. Locate the tropopause height $z_T(\lambda, \phi, t)$ at each longitude λ and latitude ϕ (we use the standard WMO definition [*WMO*, 1957]) and define the entry patch Ω_i.

[77] 2. Pulse the mixing ratio of tracer $\mathcal{G}(\mathbf{r}, t|\Omega_i, t_i)$ on patch Ω_i by setting $\mathcal{G}$ to $1/\Delta t_P$ during $t \in (t_i, t_i + \Delta t_P)$ and to zero elsewhere. (We use $\Delta t_P = 1$ day.)

[78] 3. At every time step δt for all times after the pulse $(t > t_i + \Delta t_P)$ compute the temporary field $\hat{\mathcal{G}}(t + \delta t) \equiv \mathcal{G}(t - \delta t) + T_A + T_D$, where T_A and T_D are the tracer tendencies due to advection and diffusion. (We use a leap-frog scheme to time step the tracer equation.)

[79] 4. Set $\hat{\mathcal{G}}(t + \delta t)$ to zero everywhere at and below the tropopause. Define this new field as $\mathcal{G}(t + \delta t)$.

[80] 5. Compute the flux $f(\lambda, \phi, t + \delta t|\Omega_i, t_i)$ of $\mathcal{G}$ by performing the vertical mass-weighted integral $f(\lambda, \phi, t + \delta t|\Omega_i, t_i) = \int_0^{z_T(\lambda, \phi, t)} \rho dz \hat{\mathcal{G}}(t + \delta t)/\delta t$ over the troposphere.

[81] From the flux of step 5 one obtains $f(\Omega_f, t|\Omega_i, t_i)$ simply by summing over all grid points (λ, ϕ) in Ω_f, that is, $f(\Omega_f, t|\Omega_i, t_i) = \Sigma_{(\lambda,\phi)\in\Omega_f} f(\lambda, \phi, t + \delta t|\Omega_i, t_i)$. The dimensions of f are (mass area^{-1} time^{-2}), so that f is a flux density per unit residence time, the time t at exit being $t_i + \tau$, where τ is the stratospheric residence time.

[82] **Acknowledgments.** This work was supported by a NSF grant ATM-0854711. Model integrations were performed at NCAR's Computational and Information Systems Laboratory. We thank Edwin Gerber and Darryn Waugh for discussions.

References

Andrews, D. G., J. R. Holton, and C. B. Leovy (1987), *Middle Atmosphere Dynamics*, 489 pp., Academic, Orlando, Fla.

Appenzeller, C., J. R. Holton, and K. H. Rosenlof (1996), Seasonal variation of mass transport across the tropopause, *J. Geophys. Res.*, *101*, 15,071–15,078.

Bourqui, M. S. (2006), Stratosphere-troposphere exchange from the Lagrangian perspective: A case study and method sensitivities, *Atmos. Chem. Phys.*, *6*, 2651–2670, doi:10.5194/acpd-4-3249-2004.

Chen, P. (1995), Isentropic cross-tropopause mass-exchange in the extratropics, *J. Geophys. Res.*, *100*(D8), 16,661–16,673, doi:10.1029/95JD01264.

Cooper, O. R., et al. (2005), Direct transport of midlatitude stratospheric ozone into the lower troposphere and marine boundary layer of the tropical Pacific Ocean, *J. Geophys. Res.*, *110*, D23310, doi:10.1029/2005JD005783.

Dethof A., A. O'Neill, and J. Slingo (2000), Quantification of the isentropic mass transport across the dynamical tropopause, *J. Geophys. Res.*, *105*(D10), 12,279–12,293, doi:10.1029/2000JD900127.

Gerber, E. P., and L. M. Polvani (2009), Stratosphere-troposphere coupling in a relatively simple AGCM: The importance of stratospheric variability, *J. Clim.*, *22*, 1920–1933, doi:10.1175/2008JCLI2548.1.

Gettelman, A., and A. H. Sobel (2000), Direct diagnoses of stratosphere-troposphere exchange, *J. Atmos. Sci.*, *57*, 3–16, doi:10.1175/1520-0469.

Hall, T. M., and M. Holzer (2003), Advective-diffusive mass flux and implications for stratosphere-troposphere exchange, *Geophys. Res. Lett.*, *30*(5), 1222, doi:10.1029/2002GL016419.

Hall, T. M., and R. A. Plumb (1994), Age as a diagnostic of stratospheric transport, *J. Geophys. Res.*, *99*, 1059–1070, doi:10.1029/93JD03192.

Hegglin, M. I., and T. G. Shepherd (2009), Large climate-induced changes in ultraviolet index and stratosphere-to-troposphere ozone flux, *Nat. Geosci.*, *2*, 687–691, doi:10.1038/ngeo604.

Hegglin, M. I., D. Brunner, T. Peter, P. Hoor, H. Fischer, J. Staehelin, M. Krebsbach, C. Schiller, U. Parchatka, and U. Weers (2006), Measurements of NO, NO_y, N_2O, and O_3 during SPURT: Implications for transport and chemistry in the lowermost stratosphere, *Atmos. Chem. Phys.*, *6*, 1331–1350.

Held, I. M., and M. J. Suarez (1994), A proposal for the intercomparison of the dynamical cores of atmospheric general circulation models, *Bull. Am. Meteorol. Soc.*, *75*, 1825–1830.

Holton, J. R., P. H. Haynes, M. E. McIntyre, A. R. Douglass, R. B. Rood, and L. Pfister (1995), Stratosphere-troposphere exchange, *Rev. Geophys.*, *33*, 403–439, doi:10.1029/95RG02097.

Holzer, M. (2009a), The path density of interhemispheric surface-to-surface transport. Part I: Development of the diagnostic and illustration with an analytic model, *J. Atmos. Sci.*, *66*, 2159–2171.

Holzer, M. (2009b), The path density of interhemispheric surface-to-surface transport. Part II: Transport through the troposphere and stratosphere diagnosed from NCEP data, *J. Atmos. Sci.*, *66*, 2172–2189.

Holzer, M., and T. M. Hall (2008), Tropospheric transport climate partitioned by surface origin and transit time, *J. Geophys. Res.*, *113*, D08104, doi:10.1029/2007JD009115.

Hsu, J., M. J. Prather, and O. Wild (2005), Diagnosing the stratosphere-to-troposphere flux of ozone in a chemistry transport model, *J. Geophys. Res.*, *110*, D19305, doi:10.1029/2005JD006045.

James, P., A. Stohl, C. Forster, and S. Eckhardt (2003), A 15-year climatology of stratosphere-troposphere exchange with a Lagrangian particle dispersion model: 2. Mean climate and seasonal variability, *J. Geophys. Res.*, *108*(D12), 8522, doi:10.1029/2002JD002639.

Jing, P., D. M. Cunnold, E. S. Yang, and H. J. Wang (2005), Influence of isentropic transport on seasonal ozone variations in the lower stratosphere and subtropical upper troposphere, *J. Geophys. Res.*, *110*, D10110, doi:10.1029/2004JD005416.

Kazuyuki, M., S. Watanabe, Y. Kawatani, K. Sato, Y. Tomikawa, and M. Takahashi (2010), Transport and mixing in the extratropical tropopause region in a high-vertical-resolution GCM. Part II: Relative importance of large-scale and small-scale dynamics, *J. Atmos. Sci.*, *67*, 1315–1336, doi:10.1175/2009JAS3334.1.

Kentarchos, A. S., and G. J. Roelofs (2003), A model study of stratospheric ozone in the troposphere and its contribution to tropospheric OH formation, *J. Geophys. Res.*, *108*(D12), 8517, doi:10.1029/2002JD002598.

McLandress, C., and T. Shepherd (2009), Simulated anthropogenic changes in the Brewer-Dobson circulation, including its extension to high latitudes, *J. Clim.*, *22*, 1516–1540, doi:10.1175/2008JCLI2679.1.

Morgenstern, O., and G. D. Carver (2001), Comparison of cross-tropopause transport and ozone in the upper troposphere and lower stratosphere region, *J. Geophys. Res.*, *106*(D10), 10,205–10,221, doi:10.1029/2000JD900802.

Olsen, M. A., M. R. Schoeberl, and A. R. Douglass (2004), Stratosphere-troposphere exchange of mass and ozone, *J. Geophys. Res.*, *109*, D24114, doi:10.1029/2004JD005186.

Pan, L. L., P. Konopka, and E. V. Browell (2006), Observations and model simulations of mixing near the extratropical tropopause, *J. Geophys. Res.*, *111*, D05106, doi:10.1029/2005JD006480.

Pan, L. L., J. C. Wei, D. E. Kinnison, R. R. Garcia, D. J. Wuebbles, and G. P. Brasseur (2007), A set of diagnostics for evaluating chemistry-climate models in the extratropical tropopause region, *J. Geophys. Res.*, *112*, D09316, doi:10.1029/2006JD007792.

Park, M., W. J. Randel, D. E. Kinnison, R. R. Garcia, and W. Choi (2004), Seasonal variation of methane, water vapor, and nitrogen oxides near the tropopause: Satellite observations and model simulations, *J. Geophys. Res.*, *109*, D03302, doi:10.1029/2003JD003706.

Plumb, R. A. (1996), A "tropical pipe" model of stratospheric transport, *J. Geophys. Res.*, *101*, 3957–3972.

Plumb, R. A. (2002), Stratospheric transport. *J. Meteorol. Soc. Jpn.*, *80*, 793–809.

Plumb, R. A., and J. D. Mahlman (1987), The zonally averaged transport characteristics of the GFDL general circulation/transport model, *J. Atmos. Sci.*, *44*, 298–327.

Plumb, R. A., and D. D. McConalogue (1988), On the meridional structure of long-lived tropospheric constituents, *J. Geophys. Res.*, *91*, 15,897–15,913.

Polvani, L. M., and P. J. Kushner (2002), Tropospheric response to stratospheric perturbations in a relatively simple general circulation model, *Geophys. Res. Lett.*, *29*(7), 1114, doi:10.1029/2001GL014284.

Primeau, F. W., and M. Holzer (2006), The ocean's memory of the atmosphere: Residence-time and ventilation-rate distributions of water masses, *J. Phys. Oceanogr.*, *36*, 1440–1456.

Stohl, A., N. Spichtinger-Rakowsky, P. Bonasoni, H. Feldmann, M. Memmesheimer, H. E. Scheel, T. Trickl, S. Hubener, W. Ringer, and M. Mandl (2000), The influence of stratospheric intrusions on alpine

ozone concentrations, *Atmos. Environ.*, *34*, 1323–1354, doi:10.1016/S1352-2310(99)00320-9.

Wernli, H., and M. Bourqui (2002), A Lagrangian "1-year climatology" of (deep) cross-tropopause exchange in the extratropical Northern Hemisphere, *J. Geophys. Res.*, *107*(D2), 4021, doi:10.1029/2001JD000812.

World Meteorological Organization (WMO) (1957), Meteorology a three-dimensional science: Second session of the commission for aerology, *WMO Bull.*, *4*(4), 134–138.

Zeng, G., O. Morgenstern, P. Braesicke, and J. A. Pyle (2010), Impact of stratospheric ozone recovery on tropospheric ozone and its budget, *Geophys. Res. Lett.*, *37*, L09805, doi:10.1029/2010GL042812.

M. Holzer, C. Orbe, and L. M. Polvani, Department of Applied Physics and Applied Mathematics, Columbia University, New York, NY 10027, USA. (co2203@columbia.edu)